



Cystine/glutamate antiporter xCT (SLC7A11) facilitates oncogenic RAS transformation by preserving intracellular redox balance

Jonathan K. M. Lim^{a,b}, Alberto Delaidelli^{a,b}, Sean W. Minaker^{a,b,1}, Hai-Feng Zhang^{a,b,1}, Milena Colovic^{a,c}, Hua Yang^c, Gian Luca Negri^a, Silvia von Karstedt^{d,e}, William W. Lockwood^{b,f}, Paul Schaffer^c, Gabriel Leprévier^{g,2}, and Poul H. Sorensen^{a,b,2}

^aDepartment of Molecular Oncology, BC Cancer, Vancouver V5Z 1L3, Canada; ^bDepartment of Pathology and Laboratory Medicine, University of British Columbia, Vancouver V6T 2B5, Canada; ^cLife Sciences, TRIUMF, Vancouver V6T 2A3, Canada; ^dDepartment of Translational Genomics, University Hospital of Cologne, 50931 Cologne, Germany; ^eCologne Excellence Cluster on Cellular Stress Response in Aging-Associated Diseases, University of Cologne, 50931 Cologne, Germany; ^fIntegrative Oncology, BC Cancer, Vancouver V5Z 1L3, Canada; and ^gClinic for Pediatric Oncology, Hematology and Clinical Immunology, Medical Faculty, Heinrich Heine University, 40225 Düsseldorf, Germany

Edited by Tak W. Mak, The Campbell Family Institute for Breast Cancer Research at Princess Margaret Cancer Centre, University Health Network, Toronto, ON, Canada, and approved March 27, 2019 (received for review December 14, 2018)

The RAS family of proto-oncogenes are among the most commonly mutated genes in human cancers and predict poor clinical outcome. Several mechanisms underlying oncogenic RAS transformation are well documented, including constitutive signaling through the RAF-MEK-ERK proliferative pathway as well as the PI3K-AKT prosurvival pathway. Notably, control of redox balance has also been proposed to contribute to RAS transformation. However, how homeostasis between reactive oxygen species (ROS) and antioxidants, which have opposing effects in the cell, ultimately influence RAS-mediated transformation and tumor progression is still a matter of debate and the mechanisms involved have not been fully elucidated. Here, we show that oncogenic KRAS protects fibroblasts from oxidative stress by enhancing intracellular GSH levels. Using a whole transcriptome approach, we discovered that this is attributable to transcriptional up-regulation of xCT, the gene encoding the cystine/glutamate antiporter. This is in line with the function of xCT, which mediates the uptake of cystine, a precursor for GSH biosynthesis. Moreover, our results reveal that the ETS-1 transcription factor downstream of the RAS-RAF-MEK-ERK signaling cascade directly transactivates the xCT promoter in synergy with the ATF4 endoplasmic reticulum stress-associated transcription factor. Strikingly, xCT was found to be essential for oncogenic KRAS-mediated transformation in vitro and in vivo by mitigating oxidative stress, as knock-down of xCT strongly impaired growth of tumor xenografts established from KRAS-transformed cells. Overall, this study uncovers a mechanism by which oncogenic RAS preserves intracellular redox balance and identifies an unexpected role for xCT in supporting RAS-induced transformation and tumorigenicity.

RAS | oncogene | xCT | antioxidants

The human RAS family of proto-oncogenes is comprised of HRAS, KRAS, and NRAS (1), which are among the most mutated genes in human cancers (2). RAS encodes a GTPase that relays signals from growth factor receptors to downstream signaling cascades. Mutations in RAS favor GTP binding, resulting in a constitutively active form of the protein, sufficient to transform cells and induce tumorigenesis in vivo (3). A number of mechanisms underlying RAS transformation have been proposed. These encompass constitutive induction of the proliferative RAF-MEK-ERK pathway (4) and the pleiotropic PI3K-AKT pathway to prevent apoptosis (5). Other proposed mechanisms include increases of extracellular proteases as well as increased calcium signaling (6). Notably, the control of redox balance has also been suggested to support RAS transformation. Initially, reactive oxygen species (ROS) were believed to contribute to RAS transformation as oncogenic Ras expression was shown to up-regulate the NADPH oxidase system, causing increased superoxide production (7–9). It

was also reported that mitochondrial ROS are required for K-Ras^{G12D}-induced tumorigenicity (10). More recently, several studies have demonstrated that on the contrary, activation of antioxidant pathways is necessary to support Ras transformation. Indeed, K-Ras^{G12D} induces the expression of the transcription factor Nrf2, the master regulator of intracellular antioxidant response, to support K-Ras^{G12D}-driven tumor development (11). In addition, oncogenic RAS cells undergo oncogene-directed metabolic reprogramming, in which glucose and glutamine are rechannelled to maintain cellular redox balance, ultimately contributing to tumor progression (12, 13). Thus, the role of ROS versus antioxidants in RAS transformation is still a matter of debate, and the mechanisms involved are not yet fully resolved.

A critical modulator of intracellular redox balance is the system x_c⁻ transporter, which mediates the exchange of intracellular glutamate for extracellular cystine, an essential precursor for GSH synthesis. This complex consists of xCT, a light-chain subunit that confers cystine transport function (14), and the

Significance

RAS genes are among the most mutated proto-oncogenes in human cancer. The mechanisms supporting RAS transformation are not fully understood, particularly regarding the relative contributions of oxidant versus antioxidant pathways. Here, we report that the cystine/glutamate transporter xCT is essential for RAS-induced tumorigenicity by enhancing antioxidant glutathione synthesis. Our findings uncover that RAS controls xCT transcription by downstream activation of ETS-1 to synergize with ATF4. This has clinical relevance since xCT expression is upregulated in human cancers exhibiting an activated RAS pathway. Therefore, oncogenic RAS transformation is supported by induction of an antioxidant program, highlighting xCT as a potential vulnerability for therapeutic targeting.

Author contributions: J.K.M.L., G.L., and P.H.S. designed research; J.K.M.L., A.D., S.W.M., H.-F.Z., M.C., G.L.N., S.v.K., and W.W.L. performed research; H.Y., S.v.K., W.W.L., and P.S. contributed new reagents/analytic tools; J.K.M.L. and G.L. analyzed data; and J.K.M.L., G.L., and P.H.S. wrote the paper.

The authors declare no conflict of interest.

This article is a PNAS Direct Submission.

This open access article is distributed under Creative Commons Attribution-NonCommercial-NoDerivatives License 4.0 (CC BY-NC-ND).

¹S.W.M. and H.-F.Z. contributed equally to this work.

²To whom correspondence may be addressed. Email: gabriel.leprévier@med.uni-duesseldorf.de or psor@mail.ubc.ca.

This article contains supporting information online at www.pnas.org/lookup/suppl/doi:10.1073/pnas.1821323116/-DCSupplemental.

Published online April 18, 2019.

CD98 heavy-chain subunit, which localizes system x_c^- to the plasma membrane. *xCT* expression is induced in response to ROS-inducing agents such as hydrogen peroxide and sodium arsenite, leading to enhanced GSH production (15). This is attributed to *cis*-acting transcriptional regulatory elements present in the *xCT* promoter, including an antioxidant response element (ARE) principally recognized by NRF2 (16), and the amino acid response element (AARE), which is bound by ATF4 (17), a major player in the integrated stress response and oxidative stress response. Expression of *xCT* is deregulated in multiple cancers. Indeed, overexpression of *xCT* has been reported in nonsmall cell lung cancer, breast cancer, and liver cancer and is associated with poor outcomes (18–21). Furthermore, *xCT* has been implicated in promoting tumorigenesis through its antioxidant function, which supports breast cancer cell proliferation (19), matrix invasion of glioma (22), and *in vivo* tumor growth of gastric cancer (23). These studies and others also demonstrated that genetic or pharmacological inhibition of *xCT*, such as with sulfasalazine and erastin, hold promise as a therapeutic strategy in these model systems (24–26). Significantly, it was recently revealed that *xCT* is involved in tumor initiation as it is directly repressed by p53 or BAP1 as a means to exert tumor suppression (27, 28). Nonetheless, whether *xCT* directly contributes to oncogene-driven tumorigenesis is unknown.

Here, we report that oncogenic KRAS protects fibroblasts against oxidative stress by stimulating *xCT* transcription to enhance GSH levels. Our results reveal that this is mediated downstream of the Ras-Raf-Mek-Erk pathway by the Ets-1 transcription factor which, in synergy with Atf4, directly transactivates the *xCT* promoter. Finally, our data highlight that *xCT* mediates oncogenic KRAS-mediated tumorigenesis *in vitro* and *in vivo* by maintaining the redox balance. Together, our study provides a mechanism contributing to RAS transformation and link the control of *xCT* expression to the RAS pathway.

Results

Oncogenic Transformation with KRAS Protects Fibroblasts from Oxidative Stress. To define the impact of oncogenic RAS signaling on the cellular response to oxidative stress and the mechanisms involved, we initially used 3T3 fibroblasts transformed by activated KRAS^{G12V} (3T3 KRAS^{V12}) or the ETV6-NTRK3 (EN) chimeric tyrosine kinase (3T3 EN) (29). As both oncoproteins constitutively activate Ras-Erk and PI3K-Akt signaling, we used both KRAS^{V12} and EN-transformed cell lines to avoid cell line-specific effects (30). Expression of oncogenic KRAS and EN were confirmed in the transformed fibroblasts (Fig. 1A).

To assess the impact of oncogenic KRAS and EN transformation on the susceptibility of fibroblasts to exogenous oxidative stress, we subjected the cells to increasing concentrations of hydrogen peroxide (H₂O₂) and quantified cell death. While H₂O₂ treatment induced massive cell death in nontransformed control cells (3T3 MSCV), especially at higher concentrations, 3T3 KRAS^{V12} and 3T3 EN cells were relatively protected (Fig. 1B), indicating that oncogenic transformation by KRAS and EN provide protection against oxidative stress. Similar effects were observed for mutant KRAS using a second oxidative stress inducer, diethyl maleate (DEM) (*SI Appendix*, Fig. S1A). These differences in cell death were linked to amounts of intracellular ROS; indeed, while 3T3 MSCV cells displayed higher levels of intracellular ROS under ambient conditions and showed rapid accumulation of ROS following H₂O₂ treatment (Fig. 1C) or DEM treatment (*SI Appendix*, Fig. S1B), 3T3 KRAS^{V12} cells maintained lower levels of intracellular ROS throughout these conditions. This is in line with previous work demonstrating that *KRas*^{G12D} expression actively suppresses ROS due to basal activation of the Nrf2 detoxification program (11). Similar effects were also seen with 3T3 EN cells (*SI Appendix*, Fig. S1C). This was further validated by analyzing levels of protein oxidation, which indicated that following exposure to

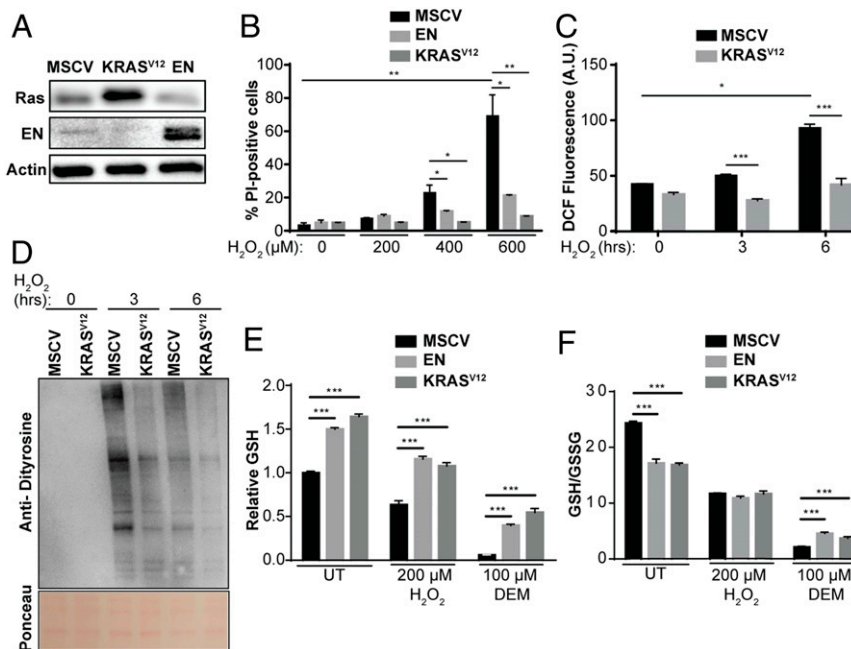


Fig. 1. Oncogenic KRAS protects fibroblasts against exogenous oxidative stress. (A) Western blot analysis of lysates obtained from 3T3 KRAS^{V12}, EN, and MSCV cells. Actin was used as a loading control. (B) 3T3 KRAS^{V12}, EN and MSCV cells were treated with indicated concentrations of H₂O₂ for 16 h, and cell death was determined by propidium iodide (PI) staining and flow cytometry ($n = 3$). (C) ROS levels in 3T3 KRAS^{V12} and MSCV cells treated with 200 μM H₂O₂ for the indicated times were determined by 6-chloromethyl-2',7'-dichlorodihydrofluorescein diacetate, acetyl ester (CM-H₂DCFDA) staining and flow cytometry ($n = 3$). (D) 3T3 KRAS^{V12} and MSCV cells were treated with 200 μM H₂O₂ for the indicated times and dityrosine levels were determined using Western blot. Ponceau was used as a loading control ($n = 3$). (E) 3T3 KRAS^{V12}, EN, and MSCV cells were treated with 200 μM H₂O₂ or 100 μM DEM for 6 h, and reduced GSH levels were determined using GSH-Glo assay (Promega) ($n = 3$). (F) 3T3 KRAS^{V12}, EN, and MSCV cells were treated with 200 μM H₂O₂ or 100 μM DEM for 6 h, and GSH/GSSG ratio was determined using GSH/GSSG-Glo assay (Promega) ($n = 3$). Where shown, data are reported as means \pm SD with indicated significance (* $P < 0.05$, ** $P < 0.01$, and *** $P < 0.005$).

H₂O₂, 3T3 MSCV cells showed higher levels of protein oxidation relative to 3T3 KRAS^{V12} cells, as measured by dityrosine levels (Fig. 1D). Moreover, together with reduced ROS, 3T3 KRAS^{V12} and EN cells consistently displayed higher reduced glutathione (GSH) levels (Fig. 1E) and higher total glutathione (GSH+GSSG) levels (SI Appendix, Fig. S1D) relative to 3T3 MSCV cells, both under ambient conditions and in response to oxidative stress by H₂O₂ or DEM treatment. Interestingly, while 3T3 KRAS^{V12} and EN cells exhibited a lower GSH/GSSG ratio relative to 3T3 MSCV cells under ambient conditions, these cells had similar GSH/GSSG ratios as 3T3 MSCV cells following H₂O₂ treatment (Fig. 1F). This suggests that in our cellular model, protection of cells against oxidative stress following oncogenic transformation with KRAS or EN may be attributed to enhanced GSH biosynthesis rather than increased GSH-GSSG recycling. Supportive of this, 3T3 KRAS^{V12} and EN cells showed higher total GSH and GSH/GSSG ratios compared with 3T3 MSCV cells when treated with DEM, which conjugates and, therefore, depletes GSH availability (Fig. 1F and SI Appendix, Fig. S1D). Together, these results suggest that oncogenic transformation with KRAS or EN protects fibroblasts against ex-

ogenous oxidative stress by preserving the redox balance and enhancing intracellular GSH capacity.

Oncogenic RAS Leads to Enhanced Induction of xCT. To uncover the mechanisms underlying KRAS^{V12}- or EN-mediated oxidative stress resistance, we performed whole-transcriptome microarray analysis of 3T3 KRAS^{V12}, EN, and MSCV cells under basal conditions (UT) and H₂O₂ treatment to identify differentially regulated transcripts potentially involved in the response to oxidative stress. When 3T3 KRAS^{V12} and 3T3 EN cells were individually analyzed following H₂O₂ treatment, we found overlap of a core of 90 probesets (corresponding to 67 unique genes) that were significantly up-regulated >twofold in both cell lines relative to 3T3 MSCV cells. Gene ontology (GO) overrepresentation analysis of these 67 genes showed significant enrichment for functional categories relating to cellular stress response and cell death, including the GO categories “cellular response to hypoxia,” “endoplasmic reticulum unfolded protein response,” and “apoptotic process” (Fig. 2A, Left). These categories comprised many up-regulated genes of the integrated stress response

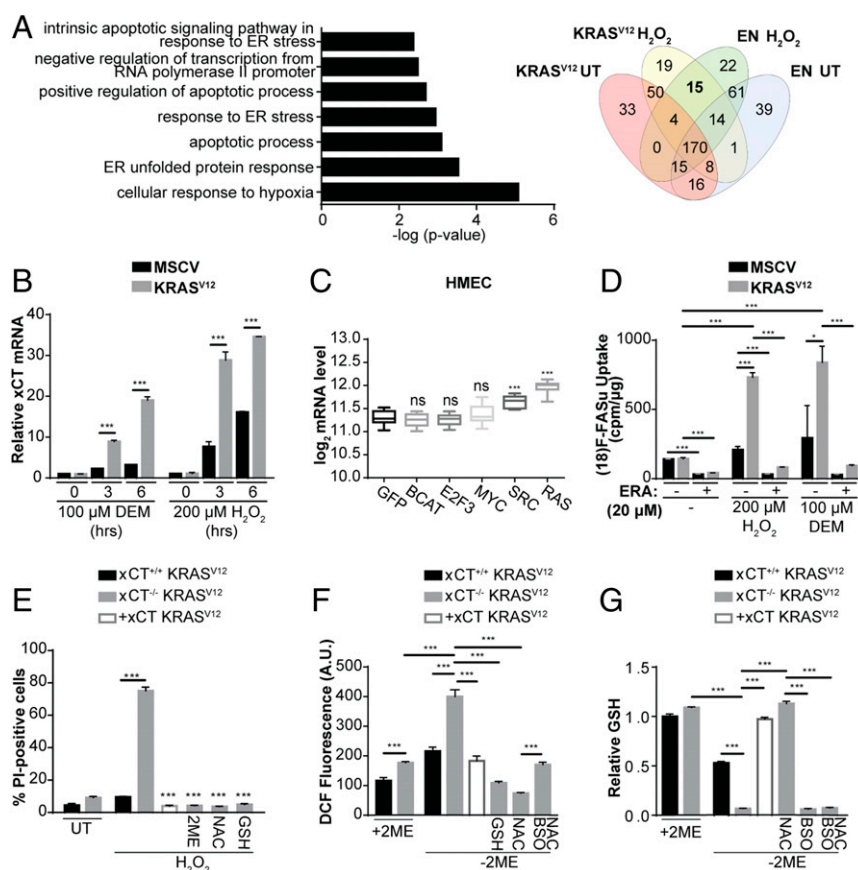


Fig. 2. Oncogenic KRAS enhances xCT induction. (A, Left) GO biological process categories overrepresented in 67 genes up-regulated in 3T3 KRAS^{V12} and 3T3 EN cells following 200 μM H₂O₂ for 3 h, for all categories with FDR < 0.10. The x axis represents the negative log of the significant score P values generated from DAVID. (A, Right) Venn diagram depicting the overlap of up-regulated genes in 3T3 KRAS^{V12} versus 3T3 MSCV and 3T3 EN cells versus MSCV under 200 μM H₂O₂ for 3 h and basal condition. (B) 3T3 KRAS^{V12} and MSCV cells were treated with 100 μM DEM or 200 μM H₂O₂ for the indicated times, and xCT mRNA levels was determined using qRT-PCR. (n = 3). (C) Expression levels of xCT in human mammary epithelial cells (HMEC) ectopically expressing indicated oncogenes or control GFP. Expression levels are displayed as log₂ of mRNA. (D) xCT activity in 3T3 KRAS^{V12} and MSCV cells treated with 200 μM H₂O₂ or 100 μM DEM for 6 h, with or without 20 μM erastin was determined by FASu uptake. FASu radioactivity was normalized to protein concentration (n = 3). (E) xCT^{+/+} KRAS^{V12} and xCT^{-/-} KRAS^{V12} cells were removed from regular media containing 2ME and treated with 200 μM H₂O₂ for 16 h; xCT^{-/-} KRAS^{V12} was rescued with 50 μM 2ME, 5 mM NAC, 5 mM GSH, or reexpression of xCT (+xCT); and cell death was determined by propidium iodide (PI) staining and flow cytometry (n = 3). (F) ROS levels in xCT^{+/+} KRAS^{V12} and xCT^{-/-} KRAS^{V12} cells removed from regular media containing 2ME and rescued with 5 mM GSH, 5 mM NAC, or 5 mM NAC and 100 μM BSO, or reexpression of xCT (+xCT) were determined by 6-chloromethyl-2',7'-dichlorodihydrofluorescein diacetate, acetyl ester (CM-H₂DCFDA) staining and flow cytometry (n = 3). (G) xCT^{+/+} KRAS^{V12} and xCT^{-/-} KRAS^{V12} cells were removed from regular media containing 2ME and rescued with 5 mM NAC or 5 mM NAC and 100 μM BSO, or reexpression of xCT and reduced GSH levels were determined using GSH-Glo assay (Promega) (n = 3). Where shown, data are reported as means ± SD with indicated significance (*P < 0.05, **P < 0.01, and ***P < 0.005).

pathway such as *Ppp1r15a*, *Atf3*, *Trib3*, *Chac1*, and *Ddit3* as well as oxidative stress response genes such as *Hmox1*, *Plk3*, and *Trp53inp1* (Dataset S1).

To better characterize individual genes uniquely up-regulated by KRAS^{V12} and EN in response to oxidative stress, we subdivided genes to identify those that were differentially up-regulated by KRAS^{V12} and EN transformation relative to control cells only under H₂O₂ treatment, and not under basal conditions. From this analysis, we identified only 15 genes with overlap across both cell lines (Fig. 2A, Right). Among these, solute carrier family 7 member 11 (*Slc7a11*; also commonly referred to as *xCT*) was of interest due to its known role in redox regulation through GSH biosynthesis. Differential expression of *xCT* mRNA was validated by qRT-PCR, confirming that while *xCT* expression was induced in all cell lines in response to DEM or H₂O₂, it was fourfold and twofold higher in 3T3 KRAS^{V12} compared with 3T3 MSCV cells at 6 h treatment with DEM and H₂O₂, respectively (Fig. 2B). To corroborate these findings in another cell type, we analyzed levels of *xCT* expression in a publicly available gene expression dataset of human mammary epithelial cells (HMEC) ectopically expressing either activated HRAS or a panel of oncogenes [*β-catenin* (*BCAT*), *E2F3*, *MYC*, or *SRC*] (31). In line with our findings, we observed that *xCT* is significantly up-regulated in HRAS^{V12} and *SRC*-transformed cells, but not in other oncogene expressing cells, compared with control GFP HMECs (Fig. 2C). Furthermore, *xCT* induction is not RAS isoform specific in 3T3 cells, as HRAS^{V12} transformation also resulted in enhanced induction of *xCT* in response to H₂O₂ (SI Appendix, Fig. S24). To further corroborate the link between RAS signaling and *xCT* expression, we used *Nras/Hras* double knockout MEFs with 4-OHT-inducible knockout of endogenous *Kras* (32). As shown in SI Appendix, Fig. S2B, in the presence of 4-OHT, the conditional *Kras* alleles become fully excised rendering the cells “Rasless.” This complete knockout of *Kras* led to a dose-dependent decrease in *xCT* expression, further linking *xCT* induction to RAS signaling (SI Appendix, Fig. S2B). In contrast, levels of GPX4, another oxidative stress response protein, were unchanged. Together, these data support the notion that oncogenic RAS pathway activation leads to induction of *xCT* expression.

We next investigated the impact of oncogenic KRAS on *xCT* activity to determine whether increased *xCT* mRNA levels led to enhanced protein activity. We opted for this approach rather than Western blotting since it has been documented that at present, all commercially available antibodies display nonspecific immunoreactivity when used to detect *xCT* protein in mouse cell lines and tissues (33). We therefore performed in vitro uptake assays of the *xCT*-specific PET tracer ¹⁸F-5-fluoroaminosuberic acid (FASu), which was developed as a diagnostic tracer of oxidative stress via system x_c⁻ activity (34, 35). In sharp contrast to nontransformed 3T3 cells, which showed no significant increase of FASu uptake following H₂O₂ and DEM exposure, 3T3 KRAS^{V12} cells consistently exhibited a five- to sixfold induction of system x_c⁻ activity in response to these compounds (Fig. 2D), in keeping with higher levels of *xCT* mRNA detected in transformed cells. FASu uptake was effectively blocked with a known *xCT* inhibitor, erastin, confirming the specificity of FASu for *xCT*. Moreover, increased FASu uptake observed in KRAS^{V12} transformed cells was not linked to altered expression of the heavy-chain subunit of system x_c⁻, i.e., CD98, as expression of the latter was similar in transformed versus nontransformed cells under basal and H₂O₂ treatment conditions (SI Appendix, Fig. S2C). This points to a major role for *xCT* in KRAS^{V12}-mediated induction of system x_c⁻ activity. Together, these results indicate that oncogenic KRAS^{V12} leads to enhanced levels of *xCT* expression and activity in response to exogenous oxidative stress.

***xCT* Mediates Oncogenic KRAS-Induced Resistance to Oxidative Stress by Preserving Redox Balance.** Given that *xCT* activity is essential to support GSH biosynthesis pathway and therefore to maintain

redox balance, we next asked whether *xCT* promotes the oxidative stress resistance conferred by oncogenic KRAS (15). To address this, we acquired mouse embryonic fibroblasts (MEFs) derived from wild-type (*xCT*^{+/+}) or *xCT*^{-/-} mice into which we stably expressed K-Ras^{V12} (36). *xCT*^{-/-} cells are routinely cultured in the reducing agent 2-mercaptoethanol (2ME), allowing these cells to circumvent the block in cysteine uptake by instead importing its reduced form, cysteine, via neutral amino acid transporters (36). Strikingly, *xCT* knockout cells transformed with K-Ras^{V12} showed marked cell death following exposure to H₂O₂ compared with wild-type cells (Fig. 2E). Similarly, knocking down *xCT* with two nonoverlapping siRNAs in 3T3 KRAS^{V12} cells increased cell death induced by H₂O₂ (SI Appendix, Fig. S2 D and E). Susceptibility to oxidative stress was reversed in MEFs and 3T3 models either by supplementation with the antioxidants GSH and NAC or with 2ME (specifically in *xCT*^{-/-} KRAS^{V12}) (Fig. 2E and SI Appendix, Fig. S2E). Further, ectopic overexpression of *xCT* in 3T3 MSCV cells phenocopied effects of oncogenic KRAS on susceptibility to H₂O₂ by protecting cells against this treatment (SI Appendix, Fig. S2F). Together, these data clearly indicate that *xCT* mediates oncogenic KRAS-induced cytoprotection against oxidative stress. This function is linked to antioxidant activity of *xCT*. 2ME depletion led to a significant increase of ROS in *xCT*^{-/-} KRAS^{V12} relative to *xCT*^{+/+} KRAS^{V12} cells, but this was reversed by reexpressing *xCT* (+*xCT* KRAS^{V12}) or by supplementation with 2ME, GSH, or NAC, but less so under cotreatment with NAC and 1-buthionine-S,R-sulfoximine (BSO), a glutamate-cysteine ligase (GCL) inhibitor (Fig. 2F). This suggests that *xCT* promotes KRAS-mediated oxidative stress resistance by providing cystine intermediates for the synthesis of GSH via GCL. Similarly, knockdown of *xCT* in 3T3 KRAS^{V12} cells was accompanied by an increase in ROS levels under both basal and H₂O₂ treatment conditions, which was also reversed by GSH or NAC, but not NAC and BSO together (SI Appendix, Fig. S2G). Consistent with this finding, knockout (Fig. 2G) or knockdown (SI Appendix, Fig. S2H) of *xCT* led to significant decreases in GSH levels under basal and oxidative stress conditions (2ME for MEFs and H₂O₂ treatment for 3T3), which could be reversed by either 2ME (specifically in *xCT*^{-/-} KRAS^{V12}) or NAC, but not NAC with BSO. Taken together, these data provide compelling evidence that *xCT* mediates resistance to oxidative stress conferred by oncogenic KRAS by providing cystine for GSH synthesis.

***xCT* Expression and Activity Are Induced by Mutant KRAS in Human Cancer Cells.** To assess regulation of *xCT* by oncogenic KRAS in human cancer cells, we analyzed various cell lines originating from mutant KRAS-driven human cancers, such as lung adenocarcinoma (LUAD), colorectal adenocarcinoma (COAD), and pancreatic ductal adenocarcinoma (PDAC). We surveyed *xCT* expression in mutant KRAS versus wild-type KRAS cancer cells from LUAD, COAD, and PDAC. Normal epithelial cells HPLID and HPDE6 from lung and pancreas, respectively, were included as controls. We found that *xCT* expression is consistently higher in mutant KRAS cancer cell lines compared with wild-type KRAS cell lines originating from the same tumor types and in normal epithelial cells (Fig. 3A), pointing to a correlation between KRAS activation and *xCT* expression in human cancer cells. To test this, we performed mutant KRAS knockdown, which markedly decreased *xCT* expression at the mRNA level in the COAD cell line SW620 (Fig. 3B), as well as at the protein level in SW620 and in the LUAD cell line H460 (Fig. 3C). Consistent with this, knockdown of mutant KRAS led to reduction of *xCT* activity (FASu uptake; Fig. 3D) and reduced GSH (Fig. 3E) in SW620 cells under basal and H₂O₂ treatment conditions. The decrease in reduced GSH levels following mutant KRAS knockdown under basal conditions was partially rescued by NAC, thereby phenocopying the effect of *xCT*

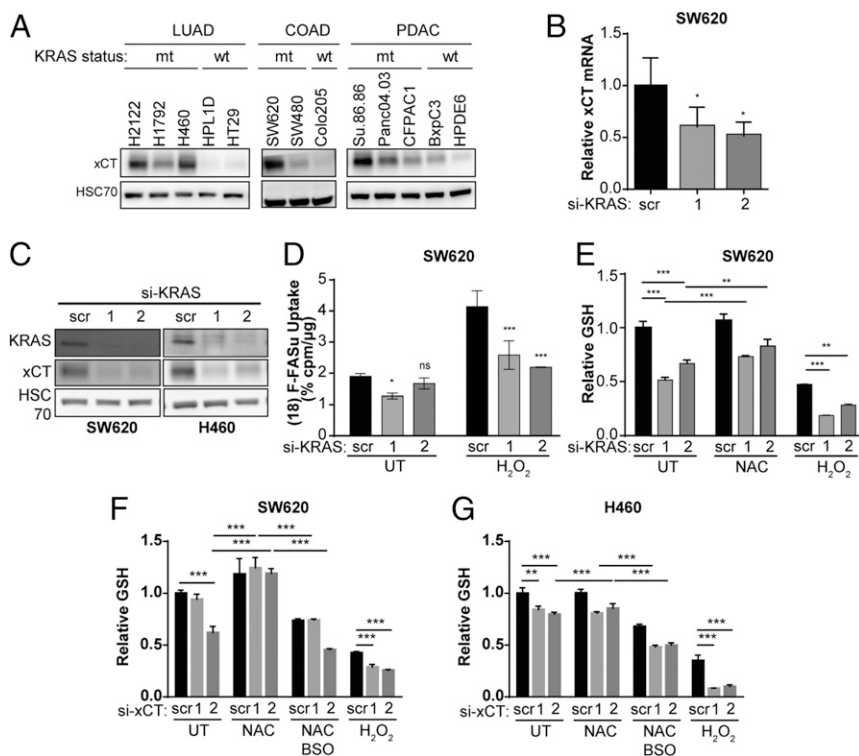


Fig. 3. Mutant KRAS regulates xCT expression and activity in human cancer cell lines. (A) Western blot analysis of xCT levels from lysates of lung adenocarcinoma (LUAD), colorectal adenocarcinoma (COAD), and pancreatic ductal adenocarcinoma (PDAC) cell lines with corresponding normal epithelial cells (HPL1D and HPDE6). HSC70 was used as a loading control. (B) SW620 cells were transfected with siRNA targeting *KRAS* or scrambled control for 72 h, and xCT mRNA levels were quantified using qRT-PCR ($n = 3$). (C) SW620 and H460 cells were transfected with siRNA targeting *KRAS* or scrambled control for 72 h, and xCT expression levels were determined using Western blot analysis. HSC70 was used as a loading control ($n = 3$). (D) xCT activity in SW620 cells transfected with siRNA targeting *KRAS* or scrambled control for 72 h and treated with 200 μM H₂O₂ for the indicated times, was determined by FASu uptake. (E) SW620 cells were transfected with siRNA targeting *KRAS* or scrambled control for 48 h, treated with 5 mM NAC or 100 μM H₂O₂ for 16 h, following which reduced GSH levels were determined using GSH-Glo assay (Promega) ($n = 3$). SW620 cells (F) and H460 cells (G) were transfected with siRNA targeting xCT or scrambled control for 48 h, treated with 5 mM NAC or 100 μM H₂O₂ for 16 h, following which reduced GSH levels were determined using GSH-Glo assay (Promega) ($n = 3$). Where shown, data are reported as means \pm SD with indicated significance (* $P < 0.05$, ** $P < 0.01$, and *** $P < 0.005$).

knockdown on reduced GSH levels as observed in 3T3 KRAS^{V12}. Consistent with 3T3 KRAS^{V12}, knockdown of xCT in SW620 cells (Fig. 3F and SI Appendix, Fig. S2 I and J) and H460 cells (Fig. 3G) led to significant decreases in GSH levels under basal and oxidative stress conditions, which could be reversed by either NAC, but not NAC in the presence of BSO, indicating that these cell lines are also dependent on xCT for GSH synthesis via GCL. Moreover, siRNA-mediated knockdown of xCT led to increased ROS levels under both basal and oxidative stress conditions (SI Appendix, Fig. S2K). Together, these results indicate that oncogenic KRAS promotes xCT expression and activity in human cancer cells to control the redox balance.

ETS-1 Mediates the Induction of xCT by Oncogenic KRAS via Synergistic Cooperation with ATF4. To elucidate how oncogenic KRAS regulates xCT expression, we analyzed transcription factor networks by performing gene set enrichment analysis (GSEA) of mRNA expression data obtained in 3T3 KRAS^{V12} versus 3T3 MSCV cells. This revealed significant enrichment of genes controlled by the transcription factor Ets-1 in oncogenic KRAS cells (SI Appendix, Fig. S3A). Ets-1 is a known substrate of ERK, downstream of the Ras-Raf-Mek pathway, but its effects on xCT transcription have not been reported. Confirming a role for the Ras-Raf-Mek pathway in xCT regulation, pharmacological inhibition of Mek (by PD184352), but not of Akt (Akt Inhibitor VIII), attenuated xCT expression in 3T3 KRAS^{V12} cells under both basal and H₂O₂ treatment conditions (SI Appendix, Fig. S3 B and C). This suggests that Ets-1 mediates KRAS^{V12} induction of xCT downstream of the Ras-Raf-Mek-Erk pathway. Indeed, knockdown of *Ets-1* with two nonoverlapping siRNAs in 3T3 KRAS^{V12} cells (SI Appendix, Fig. S3D) significantly restricted xCT induction in response to H₂O₂ treatment versus control siRNAs (Fig. 4A). Accordingly, *Ets-1* knockdown increased ROS levels in KRAS^{V12}-transformed cells under basal conditions, which was rescued by xCT overexpression or NAC supplementation, and dramatically increased ROS levels under

H₂O₂ treatment (SI Appendix, Fig. S3E). Moreover, blocking *Ets-1* expression increased sensitivity of 3T3 KRAS^{V12} cells to H₂O₂ (SI Appendix, Fig. S3F). Therefore, Ets-1 confers KRAS^{V12} cytoprotection against oxidative stress, potentially by controlling xCT expression. In human cancer cells harboring KRAS mutations, *ETS-1* knockdown similarly decreased xCT expression at both the mRNA and protein level compared with siRNA controls (Fig. 4 B and C). To corroborate this, we ectopically expressed *ETS-1* in the DLD-1 colon cancer cell line devoid of *ETS-1* expression, which was sufficient to up-regulate xCT expression at both the mRNA and protein level under H₂O₂ treatment (Fig. 4D). Together, these highlight a role for ETS-1 in mediating KRAS^{V12} induction of xCT expression.

Next, to demonstrate whether ETS-1 controls the activity of xCT promoter, we performed luciferase transactivation assays in HEK293 cells. Notably, one potential ETS-1 binding site (E1BS), 5'-TGAGGAAGCT-3' containing the consensus GGAA/T core motif at position -15 of the human xCT promoter, was detected in silico (SI Appendix, Fig. S3G). Indeed, exogenous ETS-1 activates a luciferase reporter containing the xCT promoter in a concentration-dependent manner (Fig. 4E). Furthermore, chromatin immunoprecipitation (ChIP) of 3T3 KRAS^{V12} cells revealed that endogenous Ets-1 occupies the promoter region of the xCT gene under both basal and H₂O₂ treatment conditions (Fig. 4F). This strongly supports xCT as a target gene of Ets-1. However, we noticed that the levels of total and phosphorylated Ets-1 (p-Ets-1, the active form of Ets-1; ref. 37), are unchanged following H₂O₂ exposure in 3T3 KRAS^{V12} cells (SI Appendix, Fig. S3H). This implies that while Ets-1 can activate xCT transcription downstream of KRAS signaling, there may be other mechanisms to explain how xCT expression is enhanced in response to oxidative stress. Therefore, to uncover other transcription factors potentially involved in xCT regulation specifically under oxidative stress, we employed GSEA in H₂O₂-treated versus untreated 3T3 KRAS^{V12} cells. This revealed enrichment of genes regulated by Atf4 under H₂O₂ treatment (SI Appendix, Fig. S4A) and conversely no enrichment of genes regulated

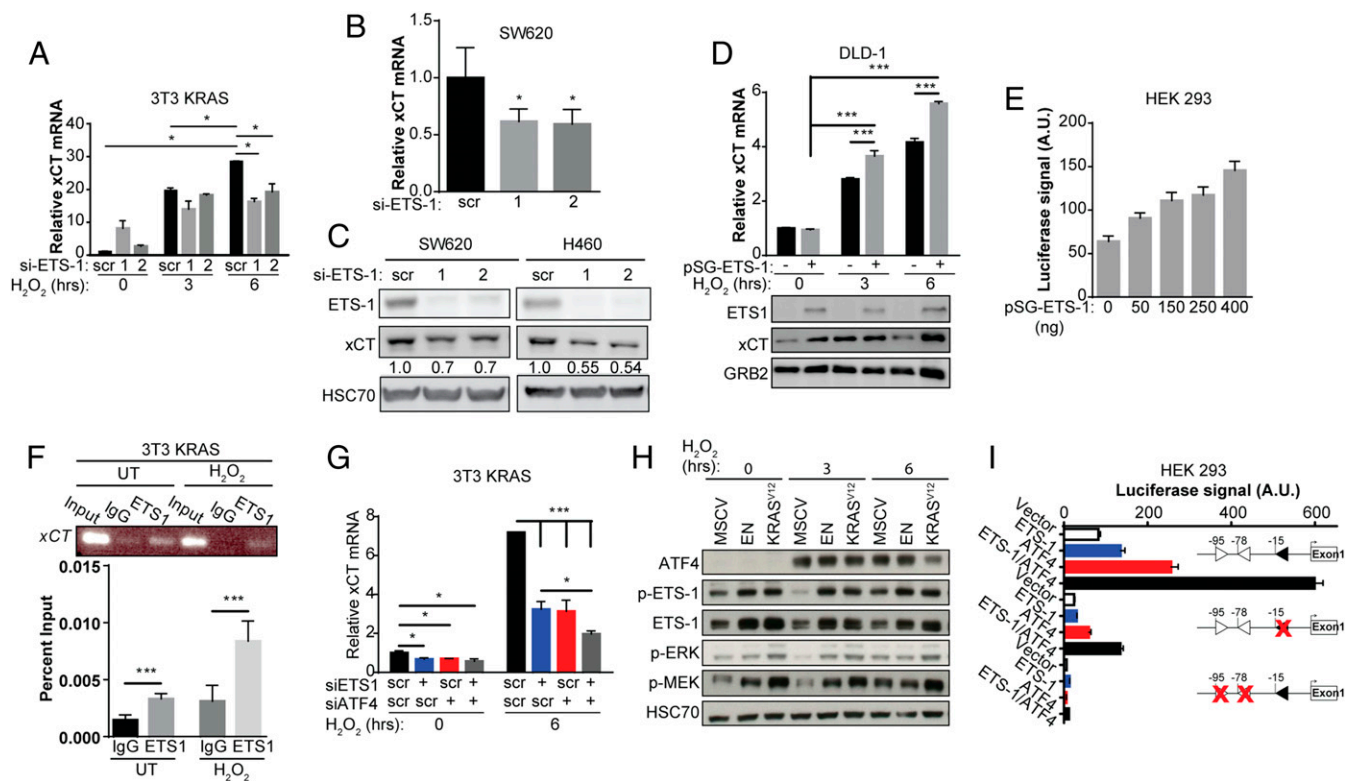


Fig. 4. ETS-1 directly transactivates *xCT* and synergizes with ATF4. (A) 3T3 KRAS^{V12} cells were transfected with siRNA targeting *Ets-1* or scrambled control for 72 h, treated with 200 μ M H₂O₂ for the indicated times, and *xCT* mRNA levels were determined by qRT-PCR ($n = 3$). (B) SW620 cells were transfected with siRNA targeting *ETS-1* for 72 h and *xCT* mRNA levels were determined by qRT-PCR ($n = 3$). (C) SW620 and H460 cells were transfected with siRNA targeting *ETS-1* or scrambled control for 72 h, and *xCT* levels were determined by Western blot analysis. HSC70 was used as a loading control ($n = 3$). (D) DLD-1 cells were transfected with *ETS-1* expression construct or control for 72 h and treated with 200 μ M H₂O₂ for the indicated times and *xCT* mRNA, and protein levels were determined by qRT-PCR and Western blot, respectively ($n = 3$). (E) HEK293 cells were transfected with luciferase construct containing *xCT* promoter and indicated concentrations of *ETS-1* expression construct for 72 h, and luciferase activity was determined by Dual-Luciferase Reporter Assay System (Promega) ($n = 3$). (F) 3T3 KRAS^{V12} cells were treated with 200 μ M H₂O₂ for 6 h, and ChIP assay was carried out. qRT-PCR was used to determine percent enrichment of *ETS-1* binding over input ($n = 3$). (G) 3T3 KRAS^{V12} cells were transfected with siRNA targeting *Ets-1*, *Atf4*, or both for 72 h, and *xCT* mRNA levels were determined by qRT-PCR ($n = 3$). (H) Western blot analysis showing ATF4, phospho-ETS-1, ETS-1 levels, phospho-ERK, and phospho-MEK in 3T3 KRAS^{V12}, EN, and MSCV cells treated with 200 μ M H₂O₂ for the indicated times. HSC70 was used as a loading control ($n = 3$). (I) HEK293 cells were transfected with *ETS-1*, *ATF4* expression construct, or both, as well as luciferase construct containing wild-type *xCT* promoter, *xCT* promoter with E1BS mutation, or *xCT* promoter with AARE mutations for 72 h. Luciferase activity was determined by the Dual-Luciferase Reporter Assay System (Promega) ($n = 3$). Where shown, data are reported as means \pm SD with indicated significance ($*P < 0.05$, $**P < 0.01$, and $***P < 0.005$).

by Ets-1. This is consistent with the established role of Atf4 as a transcriptional regulator of *xCT* expression in response to oxidative stress (17). Indeed, knockdown of *Atf4* markedly suppressed *xCT* induction (SI Appendix, Fig. S4B) and *xCT* protein expression (SI Appendix, Fig. S4C) in response to H₂O₂ in 3T3 KRAS^{V12} and H460 cells, respectively. Notably, knocking down *Ets-1* together with *Atf4* achieved a stronger suppression of *xCT* induction under oxidative stress conditions than targeting *Ets-1* or *Atf4* alone (Fig. 4G), suggesting an interplay between these two transcription factors in regulating *xCT* expression. While total and phosphorylated Ets-1 are up-regulated in KRAS^{V12}-transformed cells compared with nontransformed cells but unaffected by H₂O₂ treatment, Atf4 expression is conversely strongly induced by H₂O₂ without any differences between MSCV and KRAS^{V12} cells (Fig. 4H). These results suggest that both transcription factors may cooperate to regulate *xCT* expression in response to both oncogenic KRAS and oxidative stress, with Ets-1 being a component of RAS signaling and Atf4 being independently regulated by oxidative stress.

To determine potential cooperativity between Ets-1 and Atf4 in regulating *xCT* promoter activity, we constructed a series of *xCT* promoter constructs containing mutations in the putative E1BS at position -15 , or in the known ATF4 binding

sites (AARE) at position -95 and -78 . Ectopically expressed ETS-1 and ATF4 were able to synergistically activate the wild-type *xCT* promoter compared with the activity induced by each alone (Fig. 4I; see top bars). However, when either the E1BS alone or the Atf4 AAREs alone were mutated, activation of the luciferase reporter was strongly decreased (Fig. 4I). Moreover, association between endogenous Ets-1 and Atf4 in a putative protein-protein complex within 3T3 KRAS^{V12} cells was confirmed by coimmunoprecipitation experiments, and this association was enhanced under oxidative stress (SI Appendix, Fig. S4D). Taken together, these results provide strong evidence that ETS-1 and ATF4 synergistically transactivate the *xCT* promoter downstream of oncogenic RAS signaling and in response to oxidative stress, possibly as a cotranscriptional activating complex.

The master regulator of the oxidative stress response, Nrf2, has also previously been shown as being induced by oncogenic KRAS (11) and to control *xCT* promoter activity in response to electrophilic agents in cooperation with Atf4 (38). We therefore investigated the role of Nrf2 in Ets-1 regulation of *xCT* transcription downstream of oncogenic KRAS. We found that, at least in 3T3 fibroblasts, while Nrf2 was increased following ectopic expression of oncogenic KRAS (or EN), its levels remain unchanged following exposure to H₂O₂ (SI Appendix, Fig. S4E).

Furthermore, siRNA-mediated knockdown of Ets-1 (upper blots) or Atf4 (lower blots) failed to alter expression of Nrf2 (*SI Appendix, Fig. S4F*). Conversely, siRNA-mediated *Nrf2* knockdown did not alter Ets-1 or Atf4 expression, nor did ATF4 overexpression alter ETS-1 levels (*SI Appendix, Fig. S4G*). This indicates that Ets-1 and Nrf2 are independently regulated downstream of the Ras-Raf-Mek pathway and, therefore, likely comprise two distinct pathways controlling *xCT* promoter activity. As expected, *Nrf2* knockdown resulted in decreased *xCT* transcript levels, which interestingly could be at least partially rescued by Atf4 overexpression (*SI Appendix, Fig. S4G*). These data suggest that while Nrf2 does not regulate Ets-1 or Atf4 to control *xCT* transcription, it may potentially coregulate *xCT* promoter together with these transcription factors. Indeed, luciferase transactivation assays reveal that NRF2 exerts an additive effect with ETS1 or ATF4 or with ETS-1 and ATF4 on *xCT* promoter activity (*SI Appendix, Fig. S4H*). However, NRF2 was unable to act in synergy with these transcription factors, contrasting with the effect observed between ETS1 and ATF4. Together, our studies provide evidence that the Ras-Raf-Mek pathway controls the *xCT* promoter through Ets-1 in synergy with Atf4, but independently of the Nrf2 pathway.

***xCT* Supports Oncogenic KRAS Transformation and Tumorigenicity in Vivo.** We next asked whether *xCT* contributes to KRAS oncogenic transformation and tumorigenicity. We first performed soft agar colony formation assays and found that siRNA-mediated *xCT* silencing results in ~70% inhibition of colony formation in 3T3 KRAS^{V12} cells (Fig. 5A). Similarly, *xCT* knockout cells transformed with K-Ras^{V12} showed markedly reduced colony formation compared with wild-type cells transformed with K-Ras^{V12} (*SI Appendix, Fig. S5A*). These results were recapitulated in the human cancer cells H460 (Fig. 5B), SW620, and SW480 (*SI Appendix, Fig. S5 B and C*, respectively) harboring KRAS mutations. Moreover, pharmacological inhibition of *xCT* using the inhibitor erastin significantly impaired the ability of 3T3 KRAS^{V12} and H460 cells to form colonies (*SI Appendix, Fig. S5 D and E*). These results strongly indicate that *xCT* is essential for KRAS-mediated oncogenic transformation and maintenance of tumorigenicity in vitro. To explore the potential mechanism involved, we assessed whether *xCT* reduces oxidative stress, proposed to be critical for oncogenic transformation (39). Notably, addition of NAC partially restored the ability of *xCT*-deficient and *xCT*-targeted cells to form colonies in soft agar (Fig. 5A and B and *SI Appendix, Fig. S5 A–C*), consistent with an important role for *xCT* in supporting oncogenic KRAS-mediated transformation through its antioxidant function. To confirm that ETS-1 and ATF4 also contribute to oncogenic KRAS transformation by regulating *xCT* transcription, we carried out siRNA-mediated silencing of *ETS-1* and *ATF4* alone, or in combination. We found these to result in more than 70% inhibition of colony formation of 3T3 KRAS^{V12} cells, compared with siRNA controls, which could be partially rescued with *xCT* overexpression or supplementation with NAC (*SI Appendix, Fig. S5F*). This highlights that ETS-1 and ATF4, by regulating *xCT* transcription, can mediate oncogenic KRAS transformation.

To determine the in vivo relevance of these findings, 3T3 KRAS^{V12} cells stably expressing scr or two individual shRNAs targeting *xCT* were s.c. implanted in *nu/nu* immunocompromised mice. Tumor xenografts established from 3T3 KRAS^{V12} cells expressing *xCT*-specific shRNA were severely impaired in their growth compared with tumors established from control scr cells (Fig. 5C). This data were accompanied by dramatically improved survival of mice bearing tumors with *xCT* silencing compared with control tumors (Fig. 5D). These highlight that *xCT* is required for KRAS-mediated tumorigenesis in vivo. To determine whether the impairment of KRAS-driven tumor growth induced by *xCT* deficiency is associated with oxidative stress, we mea-

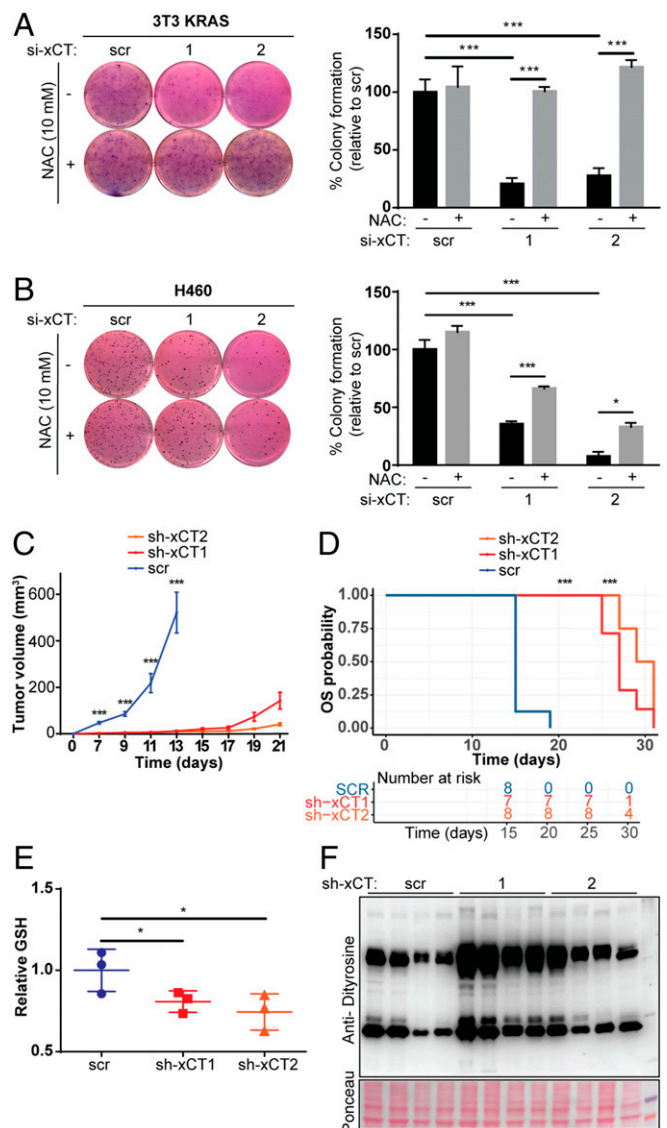


Fig. 5. *xCT* is required for oncogenic KRAS-mediated transformation and tumorigenicity. (A) 3T3 KRAS^{V12} cells were transfected with siRNA targeting *xCT* or scrambled control for 24 h and seeded into soft agar with or without 10 mM NAC for 3 wk, following which colony formation was determined by MTT staining ($n = 3$). (B) H460 cells were transfected with siRNA targeting *xCT* or scrambled control for 24 h and seeded into soft agar with or without 10 mM NAC for 3 wk, following which colony formation was determined by MTT staining ($n = 3$). (C) 3T3 KRAS^{V12} cells were transfected with shRNA targeting *xCT* or scrambled control and were s.c. implanted in *nu/nu* immunocompromised mice. Tumor volume was determined every 2 d ($n = 8$). (D) Survival of mice bearing tumors from 3T3 KRAS^{V12} cells expressing shRNA targeting *xCT* or scrambled control ($n = 8$). (E) Quantification of reduced GSH levels of tumor lysate from 3T3 KRAS^{V12} cells expressing shRNA targeting *xCT* or scrambled control using GSH-Glo assay (Promega) ($n = 8$). (F) Western blot analysis of dityrosine levels of tumor lysate from 3T3 KRAS^{V12} cells expressing shRNA targeting *xCT* or scrambled control. Where shown, data are reported as means \pm SD with indicated significance ($*P < 0.05$, $**P < 0.01$, and $***P < 0.005$).

sured GSH levels and found that tissues from *xCT*-knockdown tumors exhibited significantly reduced GSH levels compared with control tumors (Fig. 5E). Further, immunoblots performed on *xCT* knockdown tumor tissues demonstrated an increase in levels of the oxidized protein marker, Dityrosine, relative to controls, providing evidence for increased oxidative stress levels in these tumors (Fig. 5F). These data support a model whereby

xCT is critical for supporting KRAS oncogenic transformation and tumorigenicity in vitro and in vivo by increasing antioxidant capacity and mitigating oxidative stress.

High *xCT* Expression Predicts Poor Outcome in Mutant KRAS-Driven Human Tumors. We next investigated the relevance of these findings in preclinical and clinical models of RAS-driven cancers. We first interrogated mRNA expression data from genetically engineered mouse models and found that lung tumor specimens from transgenic mice expressing *Kras*^{G12D} mutant display higher levels of *xCT* mRNA compared with those from oncogenic *c-Myc*-expressing mice or from normal lung tissue (Fig. 6A). Additionally, elevated levels of *xCT* mRNA were also found in lung tumor specimens from transgenic mice expressing either *EGFR* in-frame exon 19 deletion mutant or the *EGFR*^{L858R} mutant, providing evidence that constitutively active RAS signaling in addition to expression of mutant RAS proteins are associated with *xCT* induction.

These findings were confirmed in clinical cancer specimens by analyzing publicly available gene expression data from lung and colon cancer and glioma patients. This revealed that *xCT* expression is up-regulated in patient tumors that are positive for *KRAS* mutations (Fig. 6B and C). Interestingly, *xCT* expression is also up-regulated in glioma tumors that are positive for *EGFR* amplification, further highlighting that constitutive RAS signaling is associated with *xCT* induction (Fig. 6D). Furthermore, hypergeometric analyses of gene expression datasets from TCGA LUAD, LUSC, and COAD cohorts revealed that the top 1% genes positively coexpressed with *xCT* are those that are significantly enriched in association with constitutively active MEK (SI Appendix, Fig. S6A). Similar analyses of these gene expression datasets also showed that the top 5% genes positively coexpressed with *xCT* are significantly enriched for genes controlled by the ETS-1 transcription factor (SI Appendix, Fig. S6B). Altogether, these results suggest that *xCT* is elevated downstream of overactive RAS-RAF-MEK-ERK-ETS-1 signaling axis in human tumors harboring *KRAS* mutations.

Finally, we assessed the prognostic value of *xCT* expression in colon cancer and glioma patients. We observed that high *xCT* levels correlates with poorer outcomes across all colon cancer subgroups (Fig. 6E) and in glioma patients (Fig. 6F). This is in line with previous reports in triple-negative breast cancer (20) as well as non-small cell lung cancer (18), and it suggests that *xCT* predicts poor prognosis in tumor types associated with increased RAS pathway activation. In summary, these data strongly suggest that *xCT* expression has prognostic value in *KRAS* mutant-expressing tumors, further reinforcing the link between oncogenic *KRAS* and *xCT* expression.

Discussion

Oncogenic RAS is well known to exert cytoprotective effects in tumor cells under diverse stress-inducing conditions (40–44). Here, we demonstrate that oncogenic *KRAS* directly protects cells against oxidative stress by stimulating *xCT* transcription to enhance intracellular GSH levels. This is in agreement with the role of *xCT* as an integral player in the cellular response to oxidative stress. Indeed, *xCT* is reported to enhance the antioxidant capacity of cancer cells as a means to support tumorigenicity and chemoresistance (25, 26, 45). We show using two models of oncogenic RAS signaling, namely *KRAS*^{V12} and EN-transformed cell lines, that oncogenic RAS activation promotes the transcription of *xCT* in response to oxidative stress by a synergistic cooperation between ETS-1 and ATF4. This is in keeping with previous reports that ATF4 is a transcriptional regulator of *xCT* expression in response to oxidative stress (17). While ATF4 and several other transcription factors including NRF2 and P53 are reported to control *xCT* expression, ETS-1 downstream of the RAS pathway is a previously unappreciated regulator of *xCT*. Moreover, our data suggests that while ATF4 is necessary to induce *xCT*, it is insufficient to elicit full induction of the latter, and that ETS-1 is required for a more complete response to oxidative stress. ETS-1 is known to synergize with other transcription factors to activate downstream targets (46), but to our knowledge, synergy between ETS-1 and ATF4 on promoters of a target gene has not

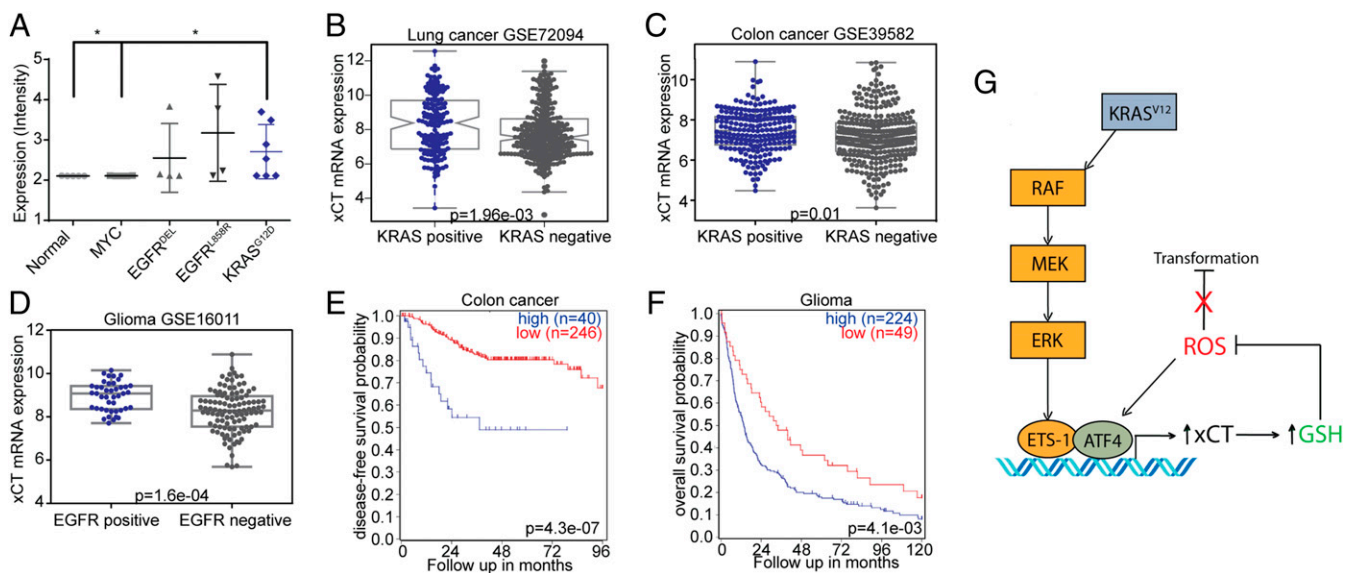


Fig. 6. Clinical relevance of *xCT* expression in mutant *KRAS*-driven tumors. (A) *xCT* expression in lung tumor specimens of transgenic mice expressing *Kras*^{G12D}, *c-Myc*, *EGFR* in-frame exon 19 deletion mutant or *EGFR*^{L858R} mutant, and normal lung tissue. Gene expression data showing *xCT* levels in lung cancer (B), colon cancer (C), and glioma (D) patient cohorts with positive or negative status for *KRAS* mutation. Survival analysis by Kaplan–Meyer plotting based on *xCT* expression in colon cancer (E) and glioma (F) patients. (G) Schematic diagram depicting oncogenic RAS activation promoting the transcription of *xCT* in response to oxidative stress by a synergistic cooperation between ETS-1 downstream of RAS-ERK signaling and ATF4. The induction of *xCT* leads to enhanced GSH biosynthesis, which is suggested to mitigate oxidative stress arising during transformation/tumorigenicity. Where shown, data are reported as means ± SD with indicated significance (**P* < 0.05, ***P* < 0.01, and ****P* < 0.005).

been documented. Given the evidence presented for a physical association between endogenous ETS-1 and ATF4, and for the binding of ETS-1 to the *xCT* promoter, both of which being enhanced under oxidative stress (SI Appendix, Fig. S4 D and F, respectively), we further speculate that this synergy may involve the direct recruitment of ETS-1 to the *xCT* promoter by ATF4, or that both transcription factors are necessary to form a functional transcriptional complex under oxidative stress. These findings represent an unanticipated mechanism to link RAS signaling to the cellular oxidative stress response. Interestingly, while oncogenic KRAS-transformed 3T3 fibroblasts show enhanced induction of *xCT* in response to oxidative stress, RAS-transformed HMECs have elevated *xCT* expression even in the basal state (Fig. 2C). This may be explained by the observation that while RAS-transformed HMECs exhibit an increase in *ATF4* expression under ambient conditions, in comparison with control HMECs (SI Appendix, Fig. S6C), this is not the case for 3T3 fibroblasts. Thus, the regulation of *xCT* by the RAS-ETS1/ATF4 cascade is observable across multiple cellular models of RAS transformation.

In ovarian carcinoma cells, *ETS-1* is a target gene of NRF2 and is up-regulated under oxidative stress (47). In contrast, we did not find evidence to support that ETS-1 expression levels are increased in response to oxidative stress or that it is downstream of NRF2 regulation in RAS-transformed 3T3 fibroblasts, which may be attributed to cell line-specific differences. Similarly, although a recent study in non-small cell lung cancer found that NRF2 up-regulates ATF4 transcription downstream of the KRAS-PI3K signaling axis in response to nutrient deprivation (42), we did not find a similar link in our study. Such regulation again may be lung tissue specific, but it may also be explained by differences in the time points investigated or the type of stress stimuli involved, as the regulation of ATF4 by NRF2 was determined at 72 h following glutamine deprivation. However, given that *xCT* is a target gene of NRF2, and NRF2 itself is transcriptionally up-regulated downstream of RAS (11), RAS-ETS1/ATF4 and RAS-ERK-NRF2 axes may form two independent signaling cascades to ultimately achieve the same output. While seemingly redundant, it is conceivable that RAS utilizes both pathways to mitigate oxidative stress and maximize tumor fitness. Two observations lend support to this idea; first, NRF2 has an additive effect on induction of *xCT* by ETS-1 and ATF4, suggesting that both the RAS-ETS-1/ATF4 and RAS-ERK-NRF2 pathways are complementary. Second, ETS-1 is activated by RAS at the posttranslational level, as a known substrate of ERK, while NRF2 is induced at the transcriptional level, providing separate mechanisms to ensure acute and sustained responses to oxidative stress through up-regulation of *xCT*. The cross-talk between these pathways and how they influence RAS-mediated antioxidant response warrants further investigation.

Our data demonstrates that *xCT* transcription is directly controlled by oncogenic RAS signaling through ETS-1, itself encoded by a proto-oncogene (48). The only other reported oncogenic mechanism controlling *xCT* expression involves oncogenic PI3K, as it was shown that this pathway suppresses *xCT* transcription and activity (49). Notably, in addition to oncogenic KRAS^{V12}, overexpression of HRAS^{V12} or ETV6-NTRK3 also induced *xCT* expression. In this regard, *xCT* overexpression may be generalizable to RAS pathway-driven cancers. This may include cancers that do not harbor RAS mutations but exhibit constitutive RAS signaling, such as lung cancer with *EGFR* mutations, glioblastoma with *NF1* mutations or *EGFR* amplification, and colon cancer and melanoma with *BRAF* mutations. Many of these tumors are notable for being highly refractory to standard chemotherapeutic agents (50–52), and therefore targeting *xCT* with pharmacological inhibitors represents an attractive therapeutic strategy to potentially sensitize RAS-driven cancers to chemotherapy. Indeed, our data lends support to this notion as preclinical models of *EGFR*-mutant lung cancer and clinical models of *EGFR*-amplified glioma were associated with

enhanced *xCT* overexpression (Fig. 6 A–D). In contrast, there was no evidence that up-regulation of *xCT* was driven by other oncogenes such as β -catenin, *E2F3*, or *MYC*, highlighting the specificity for oncogenic RAS signaling. These findings thus enhance our general understanding of how tumors up-regulate *xCT*, which is clinically relevant since it is overexpressed in multiple cancers and is a marker of poor prognosis (18–21).

The role of ROS versus antioxidants in RAS transformation is controversial, and the mechanisms involved have not been completely elucidated. We provide further evidence that antioxidants indeed contribute to RAS transformation, as *xCT* facilitates oncogenic KRAS-mediated tumorigenesis in vitro and in vivo by maintaining the redox balance. Previously proposed mechanisms of antioxidant-mediated RAS transformation include up-regulation of NRF2, the master regulator of intracellular antioxidant response, and rechanneling of glucose and glutamine into GSH and NADPH-generating metabolic pathways (11–13). Furthermore, broad evidence now shows that cancer cells that are able to initiate intrinsic antioxidant responses are selected for during tumor progression to cope with oxidative stress arising in response to oncogene activation, accumulation of genetic instability, aberrant metabolism, and mitochondrial dysfunction (53). For example, it has been observed that a subset of cancer stem cells in human and mouse mammary tumors contain lower levels of ROS and display less DNA damage relative to their nontumorigenic counterparts, due to increased GSH biosynthesis genes such as *GCLM* and *GSS* (54). In addition, GSH pathways are critical for tumor initiation, as genetic loss of *Gclm* resulted in the inability of mice to form mammary tumors (55). More recently, Truitt et al. (39) demonstrated that cancer cells hijack an eIF4E-dependent translation program that is selectively enriched for mRNAs involved in antioxidant responses to support cell survival and fuel oncogenic transformation. Therefore, while cancer cells rely on ROS induction to promote protumorigenic processes such as proliferation, they are also critically dependent on adaptive or intrinsic ROS-scavenging pathways to restrict oxidative damage that can ultimately impede tumor progression. This dependence on ROS-clearing mechanisms thus reveals a vulnerability that represents a tractable therapeutic strategy, such as the use of high-dose vitamin C to exacerbate oxidative stress by depleting GSH, thereby selectively killing *KRAS* and *BRAF*-mutated colorectal cancer cells (56). Such a strategy may also extend to targeting other steps of cancer progression, such as metastasis, as a clear role for antioxidants in promoting tumor metastasis has been shown (57–59).

In summary, our work reveals that oncogenic RAS protects tumor cells from oxidative stress by enhancing GSH via *xCT* up-regulation. We present evidence that ETS-1 synergizes with ATF4 to directly transactivate the *xCT* promoter downstream of the RAS-ERK pathway in response to oxidative stress (Fig. 6G). As such, *xCT* supports oncogenic KRAS-mediated transformation by maintaining the redox balance, presenting a candidate therapeutic target for this subset of therapy-resistant tumors.

Materials and Methods

Cell Culture. NIH 3T3 cells stably expressing EN or KRAS^{V12} were as described (60). *xCT*^{-/-} (KO) and *xCT*^{+/+} (WT) MEFs were a kind gift from Hideyo Sato (Niigata University, Niigata, Japan) and routinely cultured in DMEM supplemented with 10% FBS (36). *xCT*^{-/-} MEFs were also supplemented with 50 μ M 2-mercaptoethanol (Sigma-Aldrich). H460 and SW620 cell lines were purchased from American Type Culture Collection (Rockville, MD) and maintained in RPMI 1640 media supplemented with 10% FBS. *Nras/Hras* double knockout MEFs with 4-OHT-inducible knockout of endogenous *Kras* were kindly provided by Mariano Barbacid, National Centre for Cancer Research, Madrid (32).

Tumorigenicity Assay. Aliquots of 0.5×10^6 cells were resuspended in 200 μ L of PBS and injected s.c. into the flanks of 5- to 6-wk-old female Nu/Nu

immunodeficient mice using standard procedures. Starting from day 13 after injection, mice euthanasia was required when tumors exceeded humane practice guidelines (500 mm³). Mice were evaluated for tumor growth every 2 d until the experimental endpoints. Tumors were measured with a caliper, and volumes were estimated using the following formula: tumor length × (tumor width)² × π/6 mm³. All animal experiments underwent ethical approval from the Animal Care Committee of the University of British Columbia (A16-0050; A16-0050-A001). Full material and methods are available in *SI Appendix, Materials and Methods*.

Gene Expression of Clinical Cancer Specimens. Analyses of gene expression data from human subjects did not require approval from the institutional review board (IRB), as the data were all obtained from publicly available

databases in which each study had utilized strict human subjects protection guidelines, informed consent, and respective IRB review of protocols.

ACKNOWLEDGMENTS. We thank A. Li, J. Cran, and N. Olsen for technical assistance and D. Radloff, B. Rotblat (Ben-Gurion University), N. Cetinbas, and C. Carnie for helpful discussions. S.v.K. was supported by the German Cancer Aid Grant 70112550. G.L. was supported by Deutsche Forschungsgemeinschaft Grant LE 3751/2-1 and German Cancer Aid Grant 70112624. This work was funded in part from Canadian Institutes of Health Research Foundation Grant FDN-143280 (to P.H.S.), and from British Columbia Cancer Foundation and Mitacs Foundation Grant BC-WD 12-13-6369 through generous donations from Team Finn and other riders in the Ride to Conquer Cancer (to P.H.S.).

- Lowy DR, Willumsen BM (1993) Function and regulation of ras. *Annu Rev Biochem* 62: 851–891.
- Prior IA, Lewis PD, Mattos C (2012) A comprehensive survey of Ras mutations in cancer. *Cancer Res* 72:2457–2467.
- Downward J (2003) Targeting RAS signalling pathways in cancer therapy. *Nat Rev Cancer* 3:11–22.
- Shaulian E, Karin M (2001) AP-1 in cell proliferation and survival. *Oncogene* 20: 2390–2400.
- Datta SR, Brunet A, Greenberg ME (1999) Cellular survival: A play in three Akts. *Genes Dev* 13:2905–2927.
- Pylyayeva-Gupta Y, Grabocka E, Bar-Sagi D (2011) RAS oncogenes: Weaving a tumorigenic web. *Nat Rev Cancer* 11:761–774.
- Irani K, et al. (1997) Mitogenic signaling mediated by oxidants in Ras-transformed fibroblasts. *Science* 275:1649–1652.
- Mitsushita J, Lambeth JD, Kamata T (2004) The superoxide-generating oxidase Nox1 is functionally required for Ras oncogene transformation. *Cancer Res* 64:3580–3585.
- Park MT, et al. (2014) Novel signaling axis for ROS generation during K-Ras-induced cellular transformation. *Cell Death Differ* 21:1185–1197.
- Weinberg F, et al. (2010) Mitochondrial metabolism and ROS generation are essential for Kras-mediated tumorigenicity. *Proc Natl Acad Sci USA* 107:8788–8793.
- DeNicola GM, et al. (2011) Oncogene-induced Nrf2 transcription promotes ROS detoxification and tumorigenesis. *Nature* 475:106–109.
- Kerr EM, Gaude E, Turrell FK, Frezza C, Martins CP (2016) Mutant Kras copy number defines metabolic reprogramming and therapeutic susceptibilities. *Nature* 531:110–113.
- Son J, et al. (2013) Glutamine supports pancreatic cancer growth through a KRAS-regulated metabolic pathway. *Nature* 496:101–105.
- Sato H, Tamba M, Ishii T, Bannai S (1999) Cloning and expression of a plasma membrane cystine/glutamate exchange transporter composed of two distinct proteins. *J Biol Chem* 274:11455–11458.
- Bannai S, Sato H, Ishii T, Taketani S (1991) Enhancement of glutathione levels in mouse peritoneal macrophages by sodium arsenite, cadmium chloride and glucose/glucose oxidase. *Biochim Biophys Acta* 1092:175–179.
- Sasaki H, et al. (2002) Electrophile response element-mediated induction of the cystine/glutamate exchange transporter gene expression. *J Biol Chem* 277:44765–44771.
- Sato H, et al. (2004) Transcriptional control of cystine/glutamate transporter gene by amino acid deprivation. *Biochem Biophys Res Commun* 325:109–116.
- Ji X, et al. (2018) xCT (SLC7A11)-mediated metabolic reprogramming promotes non-small cell lung cancer progression. *Oncogene* 37:5007–5019.
- Yang Y, Yee D (2014) IGF-1 regulates redox status in breast cancer cells by activating the amino acid transport molecule xC-. *Cancer Res* 74:2295–2305.
- Timmerman LA, et al. (2013) Glutamine sensitivity analysis identifies the xCT antiporter as a common triple-negative breast tumor therapeutic target. *Cancer Cell* 24: 450–465.
- Guo W, et al. (2011) Disruption of xCT inhibits cell growth via the ROS/autophagy pathway in hepatocellular carcinoma. *Cancer Lett* 312:55–61.
- Tsuchihashi K, et al. (2016) The EGF receptor promotes the malignant potential of glioma by regulating amino acid transport system xc(-). *Cancer Res* 76:2954–2963.
- Ishimoto T, et al. (2011) CD44 variant regulates redox status in cancer cells by stabilizing the xCT subunit of system xc(-) and thereby promotes tumor growth. *Cancer Cell* 19:387–400.
- Zhang W, et al. (2012) Stromal control of cystine metabolism promotes cancer cell survival in chronic lymphocytic leukaemia. *Nat Cell Biol* 14:276–286.
- Yoshikawa M, et al. (2013) xCT inhibition depletes CD44v-expressing tumor cells that are resistant to EGFR-targeted therapy in head and neck squamous cell carcinoma. *Cancer Res* 73:1855–1866.
- Sato M, et al. (2018) The ferroptosis inducer erastin irreversibly inhibits system xc- and synergizes with cisplatin to increase cisplatin's cytotoxicity in cancer cells. *Sci Rep* 8:968.
- Jiang L, et al. (2015) Ferroptosis as a p53-mediated activity during tumour suppression. *Nature* 520:57–62.
- Zhang Y, et al. (2018) BAP1 links metabolic regulation of ferroptosis to tumour suppression. *Nat Cell Biol* 20:1181–1192.
- Knezevich SR, McFadden DE, Tao W, Lim JF, Sorensen PH (1998) A novel ETV6-NTRK3 gene fusion in congenital fibrosarcoma. *Nat Genet* 18:184–187.
- Tognon CE, et al. (2012) A tripartite complex composed of ETV6-NTRK3, IRS1 and IGF1R is required for ETV6-NTRK3-mediated membrane localization and transformation. *Oncogene* 31:1334–1340.
- Bild AH, et al. (2006) Oncogenic pathway signatures in human cancers as a guide to targeted therapies. *Nature* 439:353–357.
- Drosten M, et al. (2010) Genetic analysis of Ras signalling pathways in cell proliferation, migration and survival. *EMBO J* 29:1091–1104.
- Van Lieffering J, et al. (2016) Comparative analysis of antibodies to xCT (SLC7A11): Forewarned is forearmed. *J Comp Neurol* 524:1015–1032.
- Webster JM, et al. (2014) Functional imaging of oxidative stress with a novel PET imaging agent, 18F-5-fluoro-L-aminosuber acid. *J Nucl Med* 55:657–664.
- Yang H, et al. (2017) ¹⁸F-5-Fluoroaminosuber acid as a potential tracer to gauge oxidative stress in breast cancer models. *J Nucl Med* 58:367–373.
- Sato H, et al. (2005) Redox imbalance in cystine/glutamate transporter-deficient mice. *J Biol Chem* 280:37423–37429.
- Callaway K, Waas WF, Rainey MA, Ren P, Dalby KN (2010) Phosphorylation of the transcription factor ets-1 by ERK2: Rapid dissociation of ADP and phospho-ets-1. *Biochemistry* 49:3619–3630.
- Ye P, et al. (2014) Nrf2- and ATF4-dependent upregulation of xCT modulates the sensitivity of T24 bladder carcinoma cells to proteasome inhibition. *Mol Cell Biol* 34: 3421–3434.
- Truitt ML, et al. (2015) Differential requirements for eIF4E dose in normal development and cancer. *Cell* 162:59–71.
- Sklar MD (1988) The ras oncogenes increase the intrinsic resistance of NIH 3T3 cells to ionizing radiation. *Science* 239:645–647.
- Grabocka E, Bar-Sagi D (2016) Mutant KRAS enhances tumor cell fitness by upregulating stress granules. *Cell* 167:1803–1813.e12.
- Gwinn DM, et al. (2018) Oncogenic KRAS regulates amino acid homeostasis and asparagine biosynthesis via ATF4 and alters sensitivity to L-asparaginase. *Cancer Cell* 33: 91–107.e6.
- Guo JY, et al. (2011) Activated Ras requires autophagy to maintain oxidative metabolism and tumorigenesis. *Genes Dev* 25:460–470.
- Tao S, et al. (2014) Oncogenic KRAS confers chemoresistance by upregulating NRF2. *Cancer Res* 74:7430–7441.
- Huang Y, Dai Z, Barbacioru C, Sadée W (2005) Cystine-glutamate transporter SLC7A11 in cancer chemosensitivity and chemoresistance. *Cancer Res* 65:7446–7454.
- Dittmer J (2003) The biology of the Ets1 proto-oncogene. *Mol Cancer* 2:29.
- Wilson LA, Gemin A, Espiritu R, Singh G (2005) ets-1 is transcriptionally up-regulated by H2O2 via an antioxidant response element. *FASEB J* 19:2085–2087.
- Seth A, Papas TS (1990) The c-ets-1 proto-oncogene has oncogenic activity and is positively autoregulated. *Oncogene* 5:1761–1767.
- Lien EC, Ghisolfi L, Geck RC, Asara JM, Tokar A (2017) Oncogenic PI3K promotes methionine dependency in breast cancer cells through the cystine-glutamate antiporter xCT. *Sci Signal* 10:eaa06604.
- Eberhard DA, et al. (2005) Mutations in the epidermal growth factor receptor and in KRAS are predictive and prognostic indicators in patients with non-small-cell lung cancer treated with chemotherapy alone and in combination with erlotinib. *J Clin Oncol* 23:5900–5909.
- Jin W, et al. (2003) Roles of the PI-3K and MEK pathways in Ras-mediated chemoresistance in breast cancer cells. *Br J Cancer* 89:185–191.
- Rosell R, et al. (1995) Single-agent paclitaxel by 3-hour infusion in the treatment of non-small cell lung cancer: Links between p53 and K-ras gene status and chemosensitivity. *Semin Oncol* 22(6 Suppl 14):12–18.
- Trachootham D, Alexandre J, Huang P (2009) Targeting cancer cells by ROS-mediated mechanisms: A radical therapeutic approach? *Nat Rev Drug Discov* 8:579–591.
- Diehn M, et al. (2009) Association of reactive oxygen species levels and radioresistance in cancer stem cells. *Nature* 458:780–783.
- Harris IS, et al. (2015) Glutathione and thioredoxin antioxidant pathways synergize to drive cancer initiation and progression. *Cancer Cell* 27:211–222.
- Yun J, et al. (2015) Vitamin C selectively kills KRAS and BRAF mutant colorectal cancer cells by targeting GAPDH. *Science* 350:1391–1396.
- Piskounova E, et al. (2015) Oxidative stress inhibits distant metastasis by human melanoma cells. *Nature* 527:186–191.
- Le Gal K, et al. (2015) Antioxidants can increase melanoma metastasis in mice. *Sci Transl Med* 7:308re8.
- Wang H, et al. (2016) NRF2 activation by antioxidant antidiabetic agents accelerates tumor metastasis. *Sci Transl Med* 8:334ra351.
- Ng TL, et al. (2012) The AMPK stress response pathway mediates anoikis resistance through inhibition of mTOR and suppression of protein synthesis. *Cell Death Differ* 19:501–510.